Inorganic Chemistry

Article

pubs.acs.org/IC

Biological Studies of Chalcogenolato-Bridged Dinuclear Half-Sandwich Complexes

Justin P. Johnpeter,[†] Gajendra Gupta,[†] Jerald Mahesh Kumar,[‡] Gunda Srinivas,[‡] Narayana Nagesh,*[,‡] and Bruno Therrien*[,†]

[†]Institut de Chimie, Université de Neuchâtel, Avenue de Bellevaux 51, CH-2000 Neuchâtel, Switzerland

[‡]CSIR-Centre for Cellular and Molecular Biology, Uppal Road, Habsiguda, Hyderabad 500 007, India

ABSTRACT: A series of cationic chalcogenolato-bridged diruthenium complexes $[(\eta^6\text{-}p\text{-}MeC_6H_4Pr^i)_2Ru_2(\mu\text{-}EC_6H_5)_3]^+$ (E = S, **1**; E = Se, **2**; E = Te, **3**) has been obtained in ethanol from the reaction of $(\eta^6\text{-}p\text{-}MeC_6H_4Pr^i)_2Ru_2(\mu\text{-}Cl)_2Cl_2$ with benzenethiol, benzeneselenol, and sodium tellurophenolate, respectively. The thiolato and selenolato derivatives are isolated in good yield as the chloride salts, while the tellurolato analogue is isolated as the hexafluorophosphate salt. Similarly, the dinuclear pentamethylcyclopentadienyl (C_5Me_5) rhodium and iridium complexes $(\eta^5\text{-}C_5Me_5)_2M_2(\mu\text{-}Cl)_2Cl_2$ react with benzenethiol, benzeneselenol, and sodium tellurophenolate in ethanol to give the corresponding cationic dinuclear complexes of the general formula $[(\eta^5\text{-}C_5Me_5)_2M_2(\mu\text{-}EC_6H_5)_3]^+$ (M = Rh, E = S, **4**; E = Se, **5**; E = Te, **6**; M = Ir, E = S, **7**; E = Se, **8**; E = Te, **9**). In addition, cationic dinuclear complexes with mixed thiolato-selenolato and thiolato-tellurolato bridges have been prepared, $[(\eta^6\text{-}p\text{-}MeC_6H_4Pr^i)_2Ru_2(\mu\text{-}EC_6H_5)(\mu\text{-}SCH_2C_6H_4\text{-}p\text{-}Bu^t)_2]^+$ (E = Se, **10**; E = Te, **11**) and $[(\eta^5\text{-}C_5Me_5)_2M_2(\mu\text{-}EC_6H_5)(\mu\text{-}SCH_2C_6H_5)_2]^+$ (M = Rh, E = Se, **12**; E = Te, **13**; M = Ir, E = Se, **14**; E = Te, **15**), starting from the neutral dinuclear complexes $(\eta^6\text{-}p\text{-}MeC_6H_4Pr^i)_2Ru_2Cl_2(\mu\text{-}SCH_2C_6H_4\text{-}p\text{-}Bu^t)_2$ and $(\eta^5\text{-}C_5Me_5)_2M_2Cl_2(\mu\text{-}SCH_2C_6H_5)_2$. All complexes are highly cytotoxic showing activity in the submicromolar range. The nature of the chalcogenolato bridges seems to have an impact on the activity, while the nature of the metal center plays a minor role. Among the complexes tested, the dinuclear complexes **1**, **4**, and **7** with the thiolato bridges show the highest activity on cancer cells and the best affinity for CT-DNA as demonstrated by cell biology and biophysical experiments.

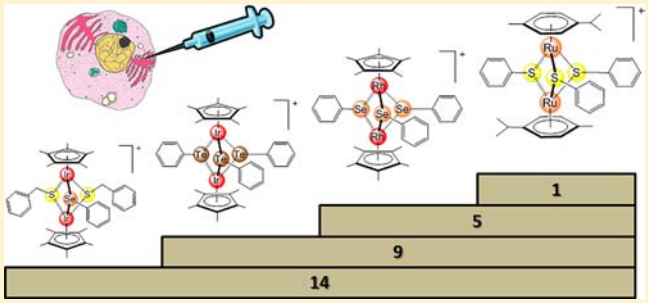

INTRODUCTION

In biology, selenium is essential to life, and it plays an important role in redox enzymatic processes.[1] At low concentrations, selenium stimulates cell growth and exhibits anticancer properties, while at higher concentrations it can induce cell death.[2] In addition, studies have shown that, in combination with cisplatin, the most successful metal-based drug,[3] selenium reduces the nephrotoxicity associated with cisplatin treatment.[4] On the other hand, the biological relevance of tellurium remains uncertain, but the potential of using tellurium derivatives as therapeutic agents has already been recognized.[5]

Recently, we have shown that the thiolato-bridged dinuclear arene ruthenium complexes of the type $[(\eta^6\text{-}p\text{-}MeC_6H_4Pr^i)_2Ru_2(\mu\text{-}SR)_3]^+$,[6] as well as the rhodium and iridium pentamethylcyclopentadienyl analogues $[(\eta^5\text{-}C_5Me_5)_2M_2(\mu\text{-}SR)_3]^+$ (M = Rh, Ir),[7] possess excellent cytotoxicity on the ovarian cancer cell lines A2780 and A2780cisR. The most active compounds show cytotoxicity against both cell lines in the submicromolar range with IC_{50} values below 0.1 μM. The high antiproliferative effect was tentatively ascribed to the presence of the thiolato-bridging groups as well as the lipophilicity and the catalytic activity of the complexes.[6] The thiolato-bridged dinuclear arene ruthenium complexes are among the most active arene ruthenium complexes evaluated so far *in vitro*.[6]

Therefore, due to the high activity of the dinuclear thiolato-bridged half-sandwich complexes and the biological relevance of selenium and tellurium, we have now prepared a series of thiolato, selenolato, and tellurolato *p*-cymene ruthenium derivatives $[(\eta^6\text{-}p\text{-}MeC_6H_4Pr^i)_2Ru_2(\mu\text{-}EC_6H_5)_3]^+$ (E = S, **1**; E = Se, **2**; E = Te, **3**), and the pentamethylcyclopentadienyl (C_5Me_5) rhodium and iridium analogues $[(\eta^5\text{-}C_5Me_5)_2M_2(\mu\text{-}EC_6H_5)_3]^+$ (M = Rh, E = S, **4**; E = Se, **5**; E = Te, **6**; M = Ir, E = S, **7**; E = Se, **8**; E = Te, **9**). In addition, a series of mixed thiolato-selenolato and thiolato-tellurolato bridged complexes has also been synthesized, $[(\eta^6\text{-}p\text{-}MeC_6H_4Pr^i)_2Ru_2(\mu\text{-}EC_6H_5)(\mu\text{-}SCH_2C_6H_4\text{-}p\text{-}Bu^t)_2]^+$ (E = Se, **10**; E = Te, **11**) and $[(\eta^5\text{-}C_5Me_5)_2M_2(\mu\text{-}EC_6H_5)(\mu\text{-}SCH_2C_6H_5)_2]^+$ (M = Rh, E = Se, **12**; E = Te, **13**; M = Ir, E = Se, **14**; E = Te, **15**). The cytotoxicity of all complexes was evaluated on normal fibroblast cells and on various cancer cells, and comparison with the parent thiolato-derivatives is discussed.

Received: September 3, 2013
Published: November 18, 2013

   dx.doi.org/10.1021/ic4022307 | *Inorg. Chem.* 2013, 52, 13663−13673

Scheme 1. Synthesis of Thiolato- and Selenolato-Bridged Complexes 1, 2, 4, 5, 7, and 8

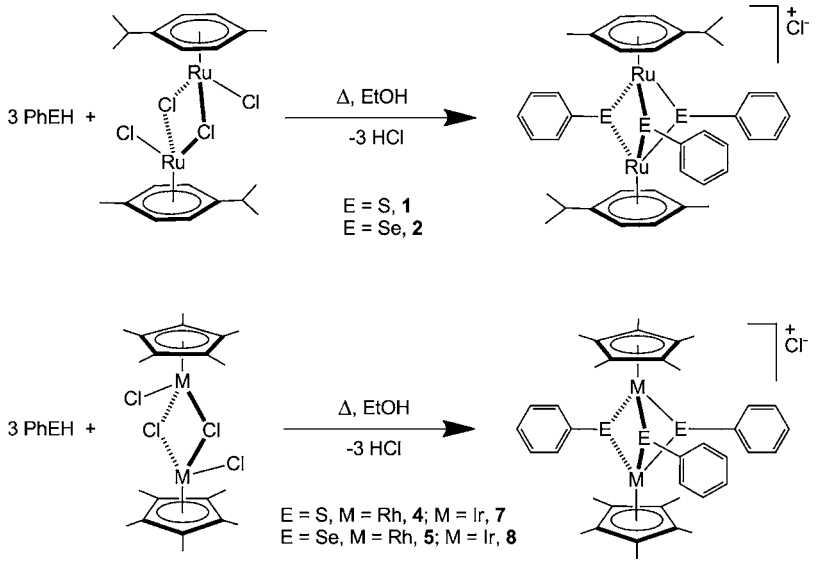

Scheme 2. Synthesis of Tellurolato-Bridged Complexes 3, 6, and 9

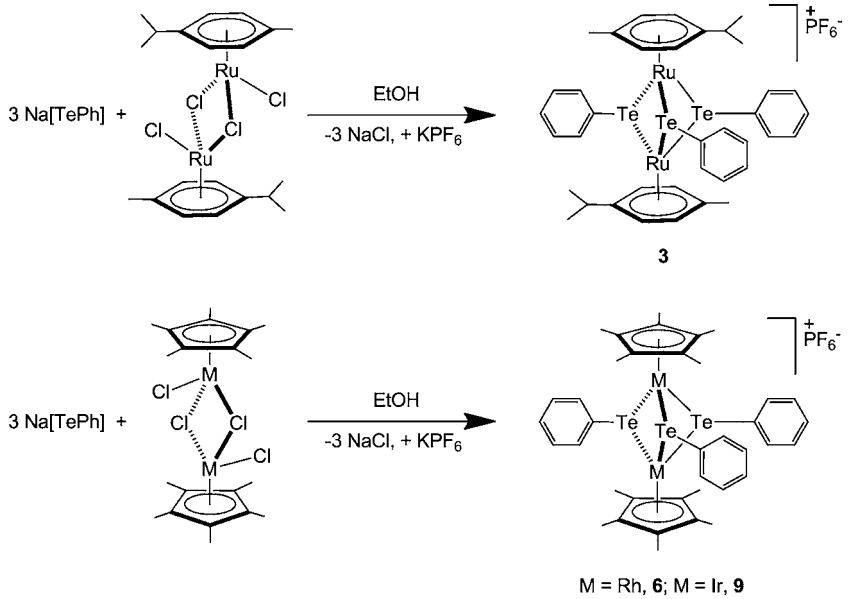

RESULTS AND DISCUSSION

Synthesis and Characterization of Complexes. Despite numerous papers dealing with thiolato-bridged dinuclear arene ruthenium complexes,[8] the only investigation of a dinuclear selenolato complex, $[(\eta^6\text{-}p\text{-}MeC_6H_4Pr^i)_2Ru_2(\mu\text{-}SeC_6H_5)_3]PF_6$, was reported 15 years ago by Mashima.[9] Low yield (19%) and difficulties with reproducibility of the reported method prompted us to prepare the desired cationic complex under new conditions (Scheme 1). Our synthetic strategy is based on the synthesis of the thiolato-bridged analogues[6] and affords $[(\eta^6\text{-}p\text{-}MeC_6H_4Pr^i)_2Ru_2(\mu\text{-}SeC_6H_5)_3]Cl$ in 66% yield after purification by column chromatography. The rhodium and iridium analogues are obtained in comparable yields following the same strategy (Scheme 1). The known thiolato-bridged *p*-cymene ruthenium complex, $[(\eta^6\text{-}p\text{-}MeC_6H_4Pr^i)_2Ru_2(\mu\text{-}SC_6H_5)_3]^+$, was also synthesized for comparison.[6a,10]

The tellurolato derivatives **3**, **6**, and **9** are prepared following an established procedure.[9] They are synthesized in ethanol from the reaction of $(\eta^6\text{-}p\text{-}MeC_6H_4Pr^i)_2Ru_2(\mu\text{-}Cl)_2Cl_2$ or $(\eta^5\text{-}C_5Me_5)_2M_2(\mu\text{-}Cl)_2Cl_2$ (M = Rh, Ir) with sodium tellurophenolate (Scheme 2): Sodium tellurophenolate being prepared *in situ* by treating diphenyl ditelluride with sodium borohydride. These complexes are all isolated as their hexafluorophosphate salts, which are obtained upon addition of 1 equiv of KPF_6 to the crude ethanolic solution, just before purification of the corresponding salts by column chromatography. The analytical data of the salt, $[(\eta^6\text{-}p\text{-}MeC_6H_4Pr^i)_2Ru_2(\mu\text{-}TeC_6H_5)_3]PF_6$, are in agreement with those reported by Mashima.[9] It is worth mentioning here that the thiolato-bridged pentamethylcyclopentadienyl rhodium complex $[(\eta^5\text{-}C_5Me_5)_2Rh_2(\mu\text{-}SC_6H_5)_3]\text{-}CF_3SO_3$[11] and the selenolato-bridged cyclopentadienyl complex $[(\eta^5\text{-}C_5H_5)_2Rh_2(\mu\text{-}SeC_6H_5)_3]Cl$[12] have been previously reported.

As previously reported for analogous *p*-cymene ruthenium complexes,[8] all ^1H NMR spectra show diastereotopic protons for the dinuclear complexes **1**−**3**, two doublets and a multiplet

dx.doi.org/10.1021/ic4022307 | Inorg. Chem. 2013, 52, 13663−13673

Scheme 3. Synthesis of the Mixed Dithiolato-Selenolato-Bridged Complexes 10, 12, and 14

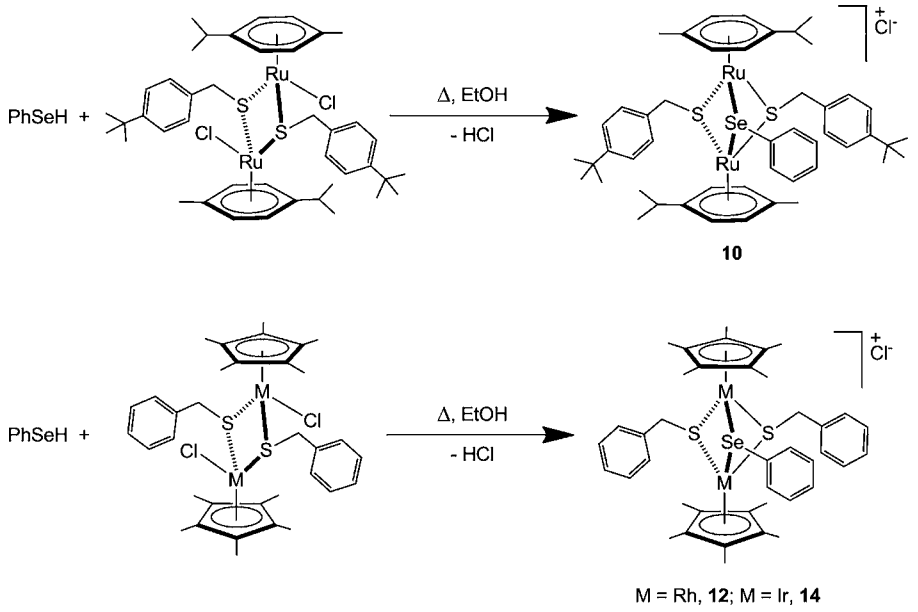

Scheme 4. Synthesis of the Mixed Dithiolato-Tellurolato-Bridged Complexes 11, 13, and 15

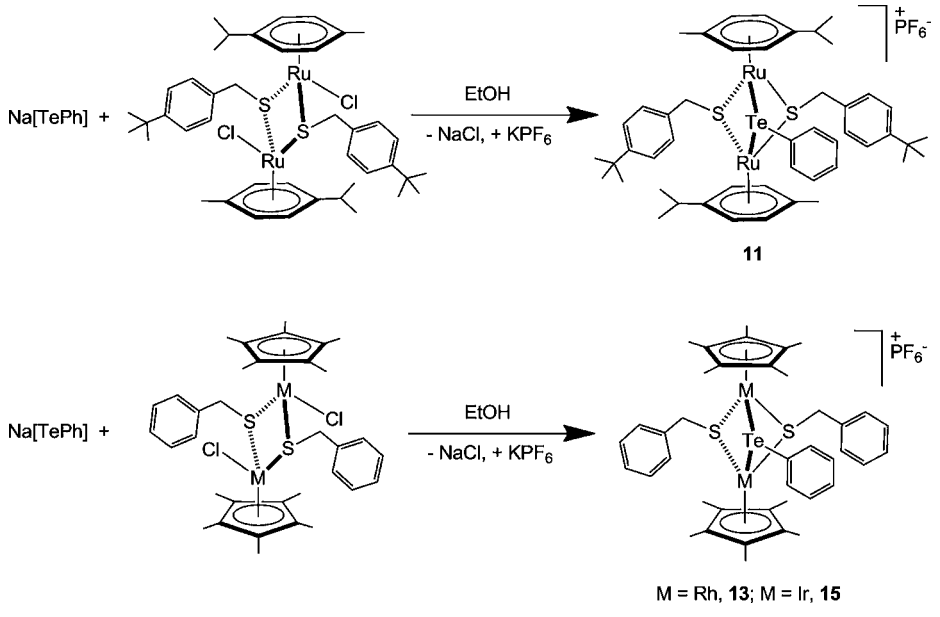

for the isopropyl group, a singlet for the methyl, four doublets for the aromatic protons of the *p*-cymene arenes, and two broad multiplets for the protons of the chalcogen-phenyl groups. The ESI mass spectrum in positive mode gives the expected cationic parent peak of $[(\eta^6\text{-}p\text{-}MeC_6H_4Pr^i)_2Ru_2(\mu\text{-}EC_6H_5)_3]^+$ at m/z = 799.1, 939.1, and 1084.3, respectively. The ^{1}H NMR spectra of the pentamethylcyclopentadienyl derivatives are much simpler, showing only an intense singlet between 1.3 and 1.8 ppm for the C_5Me_5 groups and multiplets in the aromatic region for the bridging chalcogen-phenyl groups. The ESI MS spectra show as well the cationic peaks corresponding to the intact cations in complexes **4**–**9**.

The neutral dichlorido dithiolato complexes $(\eta^6\text{-}p\text{-}MeC_6H_4Pr^i)_2Ru_2Cl_2(\mu\text{-}SCH_2C_6H_4\text{-}p\text{-}Bu^t)_2$[6b] and $(\eta^5\text{-}C_5Me_5)_2M_2Cl_2(\mu\text{-}SCH_2C_6H_5)_2$[7] react with benzeneselenol and sodium tellurophenolate in ethanol to give the mixed dithiolato-selenolato and dithiolato-tellurolato cationic dinuclear complexes $[(\eta^6\text{-}p\text{-}MeC_6H_4Pr^i)_2Ru_2(\mu\text{-}EC_6H_5)(\mu\text{-}SCH_2C_6H_4\text{-}p\text{-}Bu^t)_2]^+$ (E = Se, **10**; E = Te, **11**) and $[(\eta^5\text{-}C_5Me_5)_2M_2(\mu\text{-}EC_6H_5)(\mu\text{-}SCH_2C_6H_5)_2]^+$ (M = Rh, E = Se, **12**; E = Te, **13**; M = Ir, E = Se, **14**; E = Te, **15**) (Schemes 3 and 4).

The dithiolato-selenolato derivatives (**10**, **12**, **14**) are synthesized in ethanol at reflux from the neutral dichlorido dithiolato complexes and benzeneselenol (Scheme 3), while the dithiolato-tellurolato analogues are obtained at room temperature by adding sodium tellurophenolate to the same neutral dinuclear complexes (Scheme 4). The selenolato derivatives (**10**, **12**, **14**) are obtained as chloride salts, while the tellurolato complexes (**11**, **13**, **15**) are isolated as hexafluorophosphate salts after addition of KPF_6 to the reaction mixture.

These mixed dithiolato-selenolato and dithiolato-tellurolato complexes are extremely stable under the harsh conditions of

dx.doi.org/10.1021/ic4022307 | *Inorg. Chem.* 2013, 52, 13663–13673

Table 1. Cytotoxicity of Complexes 1−15 after 24 h Exposure to Various Cell Lines and T_m Values of the Complexes with CT-DNA

	IC_{50} values (nM)					
complex	CRL-2115	CRL-2120	MCF-7	B16F10	A549	T_m (°C)
1	935 ± 4	1078 ± 5	543 ± 5	306 ± 3	424 ± 4	75
2	965 ± 6	1082 ± 7	574 ± 6	352 ± 5	440 ± 5	66
3	950 ± 5	1074 ± 6	562 ± 4	346 ± 4	432 ± 3	68
4	965 ± 3	1172 ± 4	567 ± 6	314 ± 2	437 ± 5	70
5	987 ± 7	1354 ± 6	553 ± 4	357 ± 5	457 ± 4	64
6	976 ± 6	1287 ± 7	561 ± 5	332 ± 4	442 ± 5	66
7	1024 ± 5	1136 ± 4	582 ± 6	319 ± 5	442 ± 6	69
8	1037 ± 7	1232 ± 6	597 ± 7	358 ± 6	472 ± 5	64
9	1025 ± 8	1187 ± 8	587 ± 4	341 ± 5	456 ± 4	67
10	967 ± 7	1087 ± 7	592 ± 5	342 ± 4	445 ± 7	68
11	953 ± 5	1079 ± 8	583 ± 6	331 ± 5	432 ± 5	65
12	986 ± 7	1089 ± 7	557 ± 4	345 ± 6	446 ± 4	62
13	972 ± 5	1076 ± 8	543 ± 7	328 ± 5	439 ± 7	64
14	1028 ± 7	1254 ± 7	568 ± 6	354 ± 7	453 ± 5	63
15	1017 ± 8	1215 ± 6	552 ± 5	346 ± 5	446 ± 6	66

electrospray ionization mass spectrometry, showing the peaks corresponding to the intact cations: $[M - Cl]^+$ for complexes **10**, **12**, and **14** and $[M - PF_6]^+$ for complexes **11**, **13**, and **15** (see Experimental Section). These peaks are unambiguously assigned on the basis of their respective isotope patterns.

All selenolato-bridged derivatives **2**, **5**, **8**, **10**, **12**, and **14** were also characterized by ^{77}Se NMR. In the ^{77}Se NMR spectrum of **5** and **12** a triplet is observed, confirming the bridging nature of the selenolato ligands between two Rh atoms, with the ^{103}Rh−^{77}Se coupling constant ($^1J_{Rh-Se}$) being 38.5 and 40.4, respectively. These data are in agreement with those obtained 15 years ago by Herberhold with the analogous complex $[(\eta^5\text{-}C_5H_5)_2Rh_2(\mu\text{-}SeC_6H_5)_3]Cl$ ($^1J_{Rh-Se}$ = 43.5 Hz).[12]

Biological Studies. In order to evaluate the biological potential of these chalcogenolato-bridged dinuclear half-sandwich complexes *in vitro*, cell biology and biophysical experiments have been carried out. Stock solutions (1 mM) of complexes **1**−**15** have been prepared by dissolving the corresponding complex in Milli-Q water, and all complexes appeared to be stable for weeks in water. Effect of these complexes on normal (CRL-2115, CRL-2120) and human cancer (A549, B16F10, and MCF-7) cell lines was studied using MTT (3-(4,5-dimethyl-2-thiazoyl)-2,5-diphenyltetrazolium bromide) assays and cell count assays. Among the organometallic complexes evaluated in the initial studies, the most cytotoxic derivatives were selected and further analyzed using flow cytometry, confocal microscopy, and DNA cleavage experiments (with and without light). In order to better understand their unique intracellular activity, interaction with DNA for the selected candidates was also studied.

MTT Assays. The MTT assay is a simple, accurate, and reliable test to estimate the activity of living cells before and after addition of a biological agent.[13] Therefore, this assay was used with complexes **1**−**15** on normal (CRL-2115 and CRL-2120 fibroblasts) and human cancer (A549 lung, B16F10 melanoma and MCF-7 breast cancers) cell lines. The assay was performed at different concentrations of complexes (10 nM, 50 nM, 100 nM, 300 nM, 500 nM, 1 μM, and 2 μM), and the absorbance obtained at 570 nm was plotted against the concentration of the complex to determine the half maximal inhibitory concentration (IC_{50} value). The IC_{50} values of the complexes and the T_m (melting temperature) values obtained in the presence of CT-DNA (calf thymus DNA) are presented in Table 1, together with the corresponding standard deviations. Among the normal and cancer cell lines studied, the cytotoxic effect is higher in the B16F10 cell line, and among all complexes, compounds **1**, **4**, and **7** appear to be the most active derivatives. Indeed, the IC_{50} of **1** on the B16F10 cell line is approximately 300 nM, closely followed by complexes **4** (≈315 nM) and **7** (≈320 nM). Complexes **1**, **4**, and **7** are those with thiolato bridges, thus suggesting that the nature of the metal plays only a minor role, while the nature of the chalcogenolato bridges is somehow important. These trends are clearly seen on the B16F10 cell line.

Accordingly, complex **1** shows the strongest affinity with CT-DNA with a T_m of ≈75 °C, which is closely followed by complexes **4** (≈70 °C) and **7** (≈69 °C). Overall, all complexes interact with CT-DNA, showing T_m values higher than 62 °C. In addition, the complexes show some selectivity toward the cancerous cell lines, being less active by half on the CRL-2115 and CRL-2120 normal fibroblast cells.

Cell Viability Assays. Cell viability assays were performed to corroborate the results obtained from the MTT assays, to find the extent of cytotoxicity induced in these cell lines and to study the selectivity of the complexes between normal and cancer cells. Both normal and cancer cells were treated with the compounds at 300 nM concentrations. After 24 h of incubation, the number of viable cells was counted in normal as well as in cancer cells using a hemocytometer. From these results, it is clear that, among the complexes studied, complexes **1**, **4**, and **7** exhibit a higher cytotoxicity in cancer cells as compared to normal cells. The elevated cytotoxicity in cancer cells can be due to a higher uptake of the cationic complexes into cancer cells.[14] Among the cell lines tested, the melanoma B16F10 cells are the most affected by the presence of the complexes. Bar graphs indicating the number of viable cells in normal as well as in cancer cells after treatment with complexes **1**, **4**, and **7** are shown in Figure 1. The bar graphs which are statistically significant with p values ≤0.05 are marked with an asterisk (*).

Flow Cytometry Experiments. The results obtained from cell viability and MTT assays indicate that, among the complexes studied, complexes **1**, **4**, and **7** exhibit the highest cytotoxicity in these cancer cell lines. Therefore, to better understand the role of these complexes in cells and to find a

dx.doi.org/10.1021/ic4022307 | Inorg. Chem. 2013, 52, 13663−13673

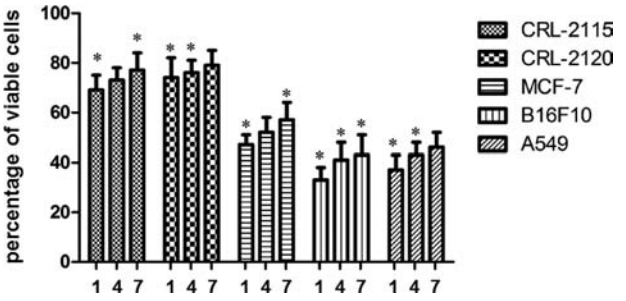

Figure 1. Cell viability assays with normal and cancer cells after 24 h of treatment with complexes **1**, **4**, and **7** at 300 nM concentrations.

plausible cause for the higher cytotoxicity and efficacy of complexes **1**, **4**, and **7**, cell cycle assays and apoptotic assays were performed using flow cytometry in the presence and absence of the complexes at their respective IC_{50} values. These tests suggest that complexes **1**, **4**, and **7** interfere with the cell cycle at the G2 stage (Figure 2). It has been previously reported that G2 arrest can enhance cytotoxicity and induce apoptosis in cells.[15] Among the complexes studied, the G2 phase inhibition is maximum in the B16F10 cells with complex **1** (24.82%) followed by complex **4** (23.05%) and complex **7** (21.37%), while untreated cells show only 14.71% of cells under the G2 phase (Table 2). Similarly, inhibition of cell cycle at the sub-G1 phase with complexes **1** (6.79%), **4** (5.59%), and **7** (4.80%) also occurs in the same order as compared to untreated cells (4.58%). These results confirm that all the complexes induce cytotoxicity followed by apoptosis induction in the cancer cell lines through G2 phase inhibition. G2 phase inhibition prevents the cells from proceeding further to the mitotic phase. The details of the cell cycle assays are presented in Figure 2.

From apoptotic assays it is clear that complex **1** possesses a higher potential to induce apoptosis (88.97%) in B16F10 cells than complexes **4** (78.82%) and **7** (69.81%) (Table 3). From the results, it is evident that **1** is quite effective in inducing higher proportion of apoptotic cells in the B16F10 cell line: more late apoptotic cells (Annexin-V+/PI+) than early apoptotic cells (Annexin-V+/PI−), whereas on treatment with complex **4** a higher percentage of early apoptotic cells are observed (Annexin-V+/PI−) over the treated cells with complexes **1** and **7**. On the other hand, when the B16F10 cells are treated with complexes **1** and **7**, more late apoptotic cells (Annexin-V+/PI+) are observed as compared to complex **4**, emphasizing the higher potential of complex **1** in inducing both early and late apoptosis in human cancer cells. The results obtained with apoptotic assays support the findings of the MTT and cell viability assays. The percentages of cell population which are in viable, necrotic, or early or late apoptotic phase

Table 2. Distribution of Cells in Various Phases of the Cell Cycle in Untreated (Control) and Treated B16F10 Cells with Complexes 1, 4, and 7

	sub-G1 (%)	G0/G1 (%)	S (%)	G2/M (%)
control	4.58	57.40	9.80	14.71
1	6.79	44.79	9.60	24.82
4	5.59	46.17	9.09	23.05
7	4.80	52.20	8.47	21.37

Table 3. Percentage of Alive, Early Apoptotic, Late Apoptotic, and Necrotic Cells in Untreated (Control) and Treated B16F10 Cells with Complexes 1, 4, and 7

	alive cells (%)	early apoptotic (%)	late apoptotic (%)	necrotic cells (%)	total apoptotic cells (%)
unstained control	99.66	0.02	0.01	0.05	low
stained control	69.54	0.02	0.10	29.33	low
1	9.16	55.82	33.15	0.78	88.97
4	20.18	68.79	10.03	0.31	78.82
7	29.30	54.50	15.31	0.41	69.81

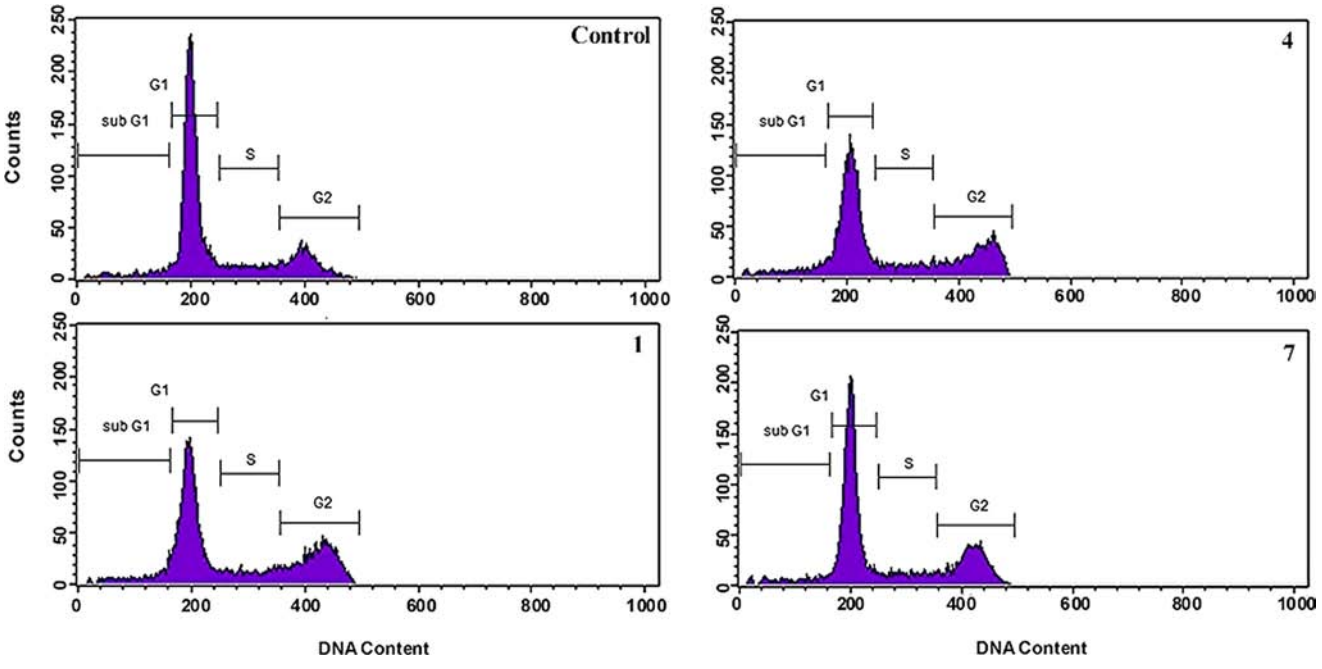

Figure 2. Untreated (control) and treated B16F10 cells with complexes **1**, **4**, and **7**. The cells were stained with propedium iodide (PI). The cellular DNA content frequency histogram and scatter plots are shown.

dx.doi.org/10.1021/ic4022307 | *Inorg. Chem.* 2013, 52, 13663−13673

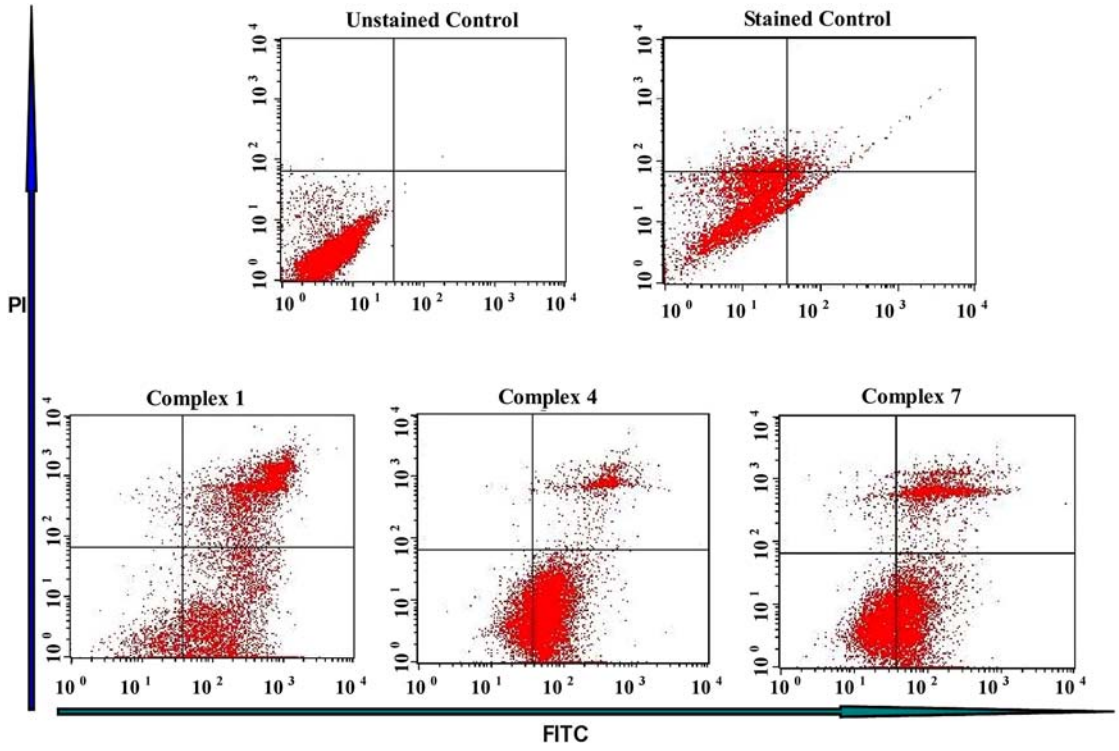

Figure 3. Untreated and treated B16F10 cells with complexes **1**, **4**, and **7**. The cells were stained with Annexin-V and propedium iodide and analyzed: viable (lower left), early apoptotic (lower right), late apoptotic (upper right), and necrotic cells (upper left).

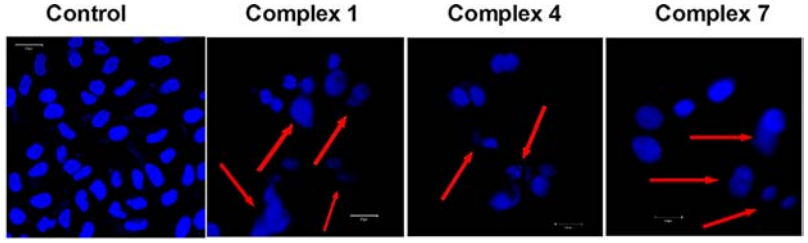

Figure 4. Confocal microscopic pictures of B16F10 cells stained with DAPI. B16F10 cells were treated with 300 nM of complexes **1**, **4**, and **7** for 24 h, red arrows mark cells undergoing apoptosis. Untreated cells were considered as control.

and in various stages of the cell cycle are shown in Table 3. The results obtained in the apoptotic assays with stained and unstained controls as well as in cells treated with complexes **1**, **4**, and **7** are presented in Figure 3.

Confocal Studies. In order to corroborate the results obtained by flow cytometry and to understand the interaction of the complexes with cellular DNA in cells, the B16F10 melanoma cells were treated with complexes **1**, **4**, and **7** for 24 h, and the state of DNA in cells after treatment was examined by staining the DNA with DAPI (4′,6-diamidino-2-phenylindole). On careful examination under a microscope of the cellular DNA of both treated and untreated B16F10 cells, it appears that complex **1** creates maximum DNA fragmentations, followed by **4** and **7**, respectively. Furthermore, the results show that complexes **1**, **4**, and **7** are capable of crossing the cell membrane barrier and interacting with the cellular DNA. The data obtained from confocal studies are shown in Figure 4. It is evident from Figure 4 that several B16F10 cells have lost their usual shape and have wrinkled upon treatment with complex **1**. The number of cells with altered shapes is comparatively less with complexes **4** and **7**. The presence of wrinkled and shrunken cells suggests that the cells are entering into the apoptosis phase.[16] Therefore, complex **1** appears to possess a higher potential to fragment cellular DNA and to induce apoptosis, which overall supports the results obtained by MTT cell viability and flow cytometry assays.

DNA Cleavage Experiments. Confocal experiments clearly show that DNAs in cells are fragmented upon treatment with complexes **1**, **4**, and **7**. It also confirms that complex **1** yields maximum DNA cleavage at its IC_{50} concentration (i.e., at around 300 nM), which was closely followed by **4** and **7**. To verify these observations, DNA cleavage experiments were carried out by incubating B16F10 cells with each complex, and the results confirm that all compounds enter the cells by crossing the cell membrane barrier and are able to interact with DNA. B16F10 cells were treated with 300 nM of complexes **1**, **4**, and **7**. DNA cleavage assay also indicates that fragmentation of DNA is prominently observed in cells treated with complex **1** followed by complexes **4** and **7**. The picture of the agarose gel after electrophoresis is shown in Figure 5.

DNA Binding Studies. The previous experiments such as flow cytometry and confocal and DNA cleavage assays suggest that complexes **1**, **4**, and **7** are efficient in inducing apoptosis in cancer cells. It is understood that the interaction with DNA is

dx.doi.org/10.1021/ic4022307 | *Inorg. Chem.* 2013, 52, 13663−13673

Figure 5. Agarose gel showing the fragmentation of DNA in B16F10 cells after treatment for 24 h with complexes **1**, **4**, and **7**. Lane 1, B16F10 cells without any treatment. Lanes 2, 3, and 4, B16F10 cells after treatment with 300 nM concentrations of complexes **1**, **4**, and **7**, respectively.

playing a major role for the development of various biological activities in cells. Interaction of these complexes with CT-DNA under *in vitro* conditions can therefore provide insight to better understand the role of these complexes in inducing apoptosis.

CT-DNA interactions with the selected complexes were studied by spectroscopic methods, circular dichroism (CD) and UV−vis spectroscopy. CD spectra of CT-DNA were recorded in biological media with complexes **1**, **4**, and **7**. The CD spectrum of CT-DNA alone exhibit a positive band at 275 nm and a negative band at around 245 nm, which is a characteristic CD signature of the right handed B form of DNA.[17] Among the studied complexes, **1** exhibits hyperchromicity of the positive CD band at 275 nm, indicating its potential to stabilize DNA upon interaction. On the other hand, with complexes **4** and **7**, the intensity of the CD bands at 275 nm exhibits a hypochromic effect indicating its role in unwinding CT-DNA. The CD spectra obtained on interaction with complexes **1**, **4**, and **7** with CT-DNA at a 1:1 stoichiometry are shown in Figure 6.

The UV−vis spectrum of complex **1** shows an absorption peak at 230 nm. On addition of CT-DNA, the soret band at 230 nm exhibits hypochromicity (about 10−15%) and shifts to 263 nm (about 33 nm bathochromic shift). Hypochromicity of the soret band occurs due to interaction between the electronic

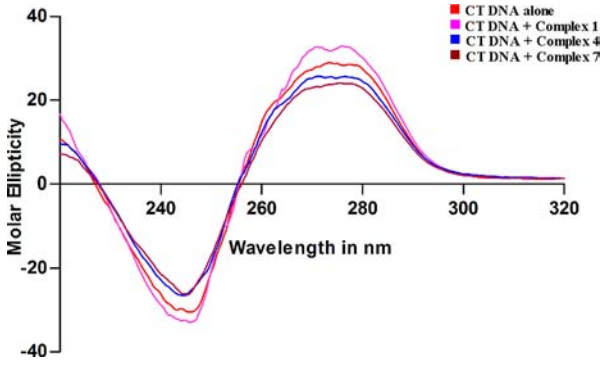

Figure 6. CD spectra obtained when complexes **1**, **4**, and **7** interact with CT-DNA. The spectra are labeled accordingly, and the corresponding samples are shown as an inset. The CD spectra were recorded twice and averaged to limit experimental errors.

states of the cationic complex and those of the DNA bases,[18] whereas a bathochromic shift is associated with the decrease in the energy gap between the highest occupied molecular orbital (HOMO) and the lowest unoccupied molecular orbital (LUMO).[19] In general, hypochromicity and bathochromic shifts indicate that molecules bind to the DNA-helix by an intercalative mode through π-stacking interactions of the aromatic chromophore of the complex between DNA bases.[20] An isosbestic point is also observed around 240 nm, and it is not a single sharp point, thus suggesting that the interaction between complex **1** and CT-DNA takes place in multiple steps, and at a given time more than one species exist at equilibrium (Figure 7A). The UV−vis spectra of complexes **4** and **7** show two absorption bands at 230−263 nm and 230−325 nm, respectively (Figures 7B and 7C). On addition of CT-DNA, the soret bands exhibit hypochromicity. The extent of hypochromicity of the soret band is an indication of strength of the ligand intercalation to DNA.[21] From Figures 7B and 7C, it is also clear that the soret band of **7** at 230 nm shows higher hypochromicity as compared to complex **4**. This suggests that complex **7** has a better interaction with DNA and unwinds the double helical structure more efficiently than **4**.[22] The UV−vis absorption spectra of CT-DNA obtained in the presence of complexes **1**, **4**, and **7** are shown in Figure 7.

DNA Photocleavage Studies. Photocleavage experiments were carried out to assess the potential of complexes **1**, **4**, and **7** to generate reactive oxygen species (ROS) on irradiation under UV light. The cleavage of DNA can be considered as a measurement of the ROS generated by each complex. If the scission occurs on one strand, the supercoiled form (Form I) will be converted to the relaxed circular form (Form II). In Figure 8, lanes 2, 3, and 4 show the gel electrophoresis separation of pBR322 DNA in the presence of complexes **1**, **4**, and **7**, respectively, after 1 h irradiation with UV light (365 nm). Each lane (2, 3, and 4) shows a slow moving band corresponding to the relaxed circular form of DNA (Form II). On the other hand, the control sample (pBR322 DNA solution alone, lane 1) and the pBR322 plasmid DNA with complexes **1**, **4**, and **7** (100 μM, lanes 5, 6 and 7) incubated with a known ROS quencher (100 μM of NaN_3) failed to show the slow moving band (Form II). These results indicate that complexes **1**, **4**, and **7** generate ROS under UV light (365 nm) and can cleave DNA. In the presence of 100 μM NaN_3, the DNA cleavage activity is significantly reduced, suggesting that NaN_3 inhibits the DNA cleavage activity of the complexes. From Figure 8, it is also evident that the DNA band intensity of relaxed circular form (form II) is higher in the presence of complex **1**, indicating its higher potential to cleave DNA by generating more ROS as compared to complexes **4** and **7**. Indeed, from this photocleavage study, the ROS generating ability of the complexes under UV light is in the order **1** > **4** > **7**, which is in perfect agreement with the DNA cleavage activity observed previously.

CONCLUSION

There were 15 chalcogenolato-bridged diruthenium, dirhodium, and diiridium complexes prepared and characterized. The biological activity of the complexes has been evaluated *in vitro* on normal (CRL-2115, CRL-2120) and human cancer (A549, B16F10, and MCF-7) cell lines. All complexes are highly cytotoxic showing activity in the submicromolar range with even some selectivity for cancer cells over normal fibroblast cells. Interestingly, the nature of the chalcogenolato bridges

dx.doi.org/10.1021/ic4022307 | *Inorg. Chem.* 2013, 52, 13663−13673

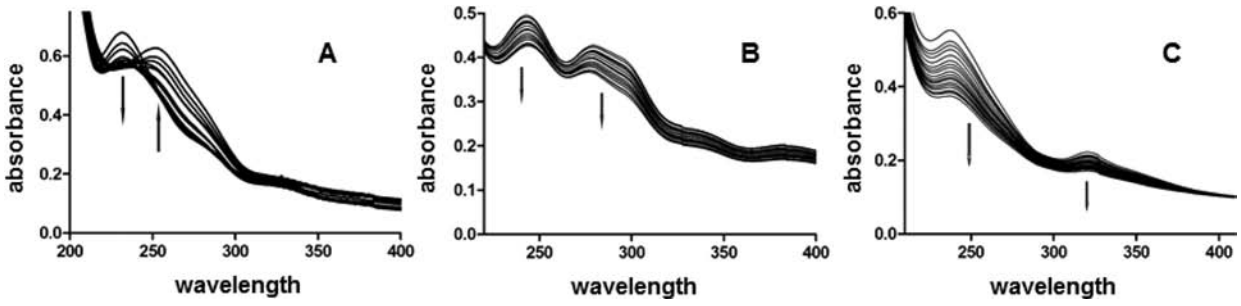

Figure 7. UV−vis spectra obtained on titrating CT-DNA with complexes **1** (A), **4** (B), and **7** (C). UV−vis spectra were recorded twice and averaged to limit experimental errors.

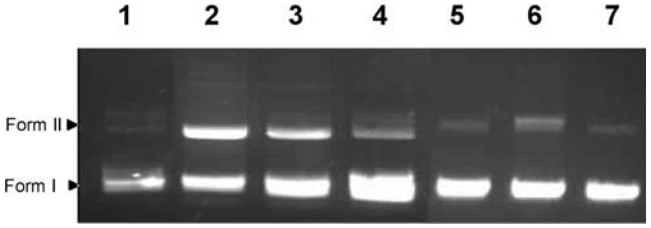

Figure 8. Agarose gel electrophoresis (0.8%, w/v) showing the UV light (365 nm) photocleavage of pBR322 plasmid DNA with complexes **1**, **4**, and **7** (100 μM) (lanes 2, 3, and 4) and in the presence of NaN_3 (100 μM) and complexes **1**, **4**, and **7** (100 μM) (lanes 5, 6, and 7), while lane 1 is the pBR322 plasmid DNA alone.

seems to have an impact on the activity, with the complexes with the thiolato bridges being slightly more cytotoxic than the selenolato and tellurolato analogues. Additionally, the nature of the metal centers appears to have a modest impact on the activity: The ruthenium derivatives are more active by a few nanomolar on all cell lines tested. The best candidates were further studied by flow cytometry, showing that the complexes can induce early and late apoptosis in B16F10 cancer cells. In addition, all complexes show strong interaction with DNA, a potential target for these complexes. Overall, these results confirm that the thiolato-bridged dinuclear half-sandwich complexes are very promising anticancer agents and deserve more biological studies.

EXPERIMENTAL SECTION

General. The starting material $(\eta^6\text{-}p\text{-}MeC_6H_4Pr^i)_2Ru_2(\mu\text{-}Cl)_2Cl_2$,[23] $(\eta^5\text{-}C_5Me_5)_2Rh_2(\mu\text{-}Cl)_2Cl_2$,[24] $(\eta^5\text{-}C_5Me_5)_2Ir_2(\mu\text{-}Cl)_2Cl_2$,[24] $(\eta^6\text{-}p\text{-}MeC_6H_4Pr^i)_2Ru_2Cl_2(\mu\text{-}SCH_2C_6H_4\text{-}p\text{-}Bu^t)_2$,[6b] $(\eta^5\text{-}C_5Me_5)_2Rh_2Cl_2(\mu\text{-}SCH_2C_6H_5)_2$,[7] and $(\eta^5\text{-}C_5Me_5)_2Ir_2Cl_2(\mu\text{-}SCH_2C_6H_5)_2$[25] were prepared according to published methods. All other reagents were purchased from Sigma-Aldrich and were used without further purification. The ^1H, ^{13}C, $^{31}P\{^1H\}$, and $^{77}Se\{^1H\}$ NMR spectra were recorded on a Bruker AMX 400 MHz spectrometer using the residual protonated solvent or $SeMe_2$ as internal standard . Electrospray mass spectra were obtained in positive-ion mode with an LCQ Finnigan mass spectrometer. Elemental analyses were performed by the Mikroelementarisches Laboratorium, ETH Zürich. Column chromatography was performed using silica gel 60 (63−200, 60 Å, Brunschwig).

*Preparation of Chalcogenolato-Bridged Dinuclear Complexes (**1**−**9**). Synthesis of $[(\eta^6\text{-}p\text{-}MeC_6H_4Pr^i)_2Ru_2(\mu\text{-}SC_6H_5)_3]Cl$ (**1**), $[(\eta^6\text{-}p\text{-}MeC_6H_4Pr^i)_2Ru_2(\mu\text{-}SeC_6H_5)_3]Cl$ (**2**), $[(\eta^5\text{-}C_5Me_5)_2Rh_2(\mu\text{-}SC_6H_5)_3]Cl$ (**4**), $[(\eta^5\text{-}C_5Me_5)_2Rh_2(\mu\text{-}SeC_6H_5)_3]Cl$ (**5**), $[(\eta^5\text{-}C_5Me_5)_2Ir_2(\mu\text{-}SC_6H_5)_3]Cl$ (**7**), and $[(\eta^5\text{-}C_5Me_5)_2Ir_2(\mu\text{-}SeC_6H_5)_3]Cl$ (**8**).* The dinuclear dichlorido complexes $(\eta^6\text{-}p\text{-}MeC_6H_4Pr^i)_2Ru_2(\mu\text{-}Cl)_2Cl_2$ (0.16 mmol, 100 mg for **1** and **2**), $(\eta^5\text{-}C_5Me_5)_2Rh_2(\mu\text{-}Cl)_2Cl_2$ (0.16 mmol, 100 mg for **4** and **5**), or $(\eta^5\text{-}C_5Me_5)_2Ir_2(\mu\text{-}Cl)_2Cl_2$ (0.13 mmol, 100 mg for **7** and **8**) were dissolved in technical-grade ethanol (20 mL). An ethanolic solution (2.5 mL) of benzenethiol (0.50 mmol, 50 μL for **1**; 0.48 mmol, 49 μL for **4**; 0.38 mmol, 38 μL for **7**) or an ethanolic solution (2.5 mL) of benzeneselenol (0.49 mmol, 52 μL for **2**; 0.48 mmol, 52 μL for **5**; 0.38 mmol, 40 μL for **8**) were added dropwise to the reaction mixture. Then, the reaction was carried out at reflux for 15 h. Then, ethanol was evaporated, and the final dinuclear complexes (**1**, **2**, **4**, **5**, **7**, and **8**) were isolated from the residue by precipitation from a dichloromethane/diethyl ether mixture. In order to improve the purity, the crude products were subjected to column chromatography on silica gel using a 95/5 dichloromethane/ethanol mixture as eluent. The second fraction was collected and evaporated and the solid dried under vacuum.

*Synthesis of $[(\eta^6\text{-}p\text{-}MeC_6H_4Pr^i)_2Ru_2(\mu\text{-}TeC_6H_5)_3]PF_6$ (**3**), $[(\eta^5\text{-}C_5Me_5)_2Rh_2(\mu\text{-}TeC_6H_5)_3]PF_6$ (**6**), and $[(\eta^5\text{-}C_5Me_5)_2Ir_2(\mu\text{-}TeC_6H_5)_3]PF_6$ (**9**).* The dinuclear dichlorido complexes $(\eta^6\text{-}p\text{-}MeC_6H_4Pr^i)_2Ru_2(\mu\text{-}Cl)_2Cl_2$ (0.13 mmol, 79 mg for **3**), $(\eta^5\text{-}C_5Me_5)_2Rh_2(\mu\text{-}Cl)_2Cl_2$ (0.16 mmol, 100 mg for **6**), or $(\eta^5\text{-}C_5Me_5)_2Ir_2(\mu\text{-}Cl)_2Cl_2$ (0.07 mmol, 58 mg for **9**) were dissolved in technical-grade ethanol (25 mL) and added to an ethanolic solution of sodium tellurophenolate, which was prepared by the treatment of diphenyl ditelluride (0.32 mmol, 132 mg for **3**; 0.48 mmol, 197 mg for **6**; 0.22 mmol, 89 mg for **9**) with sodium borohydride (0.37 mmol, 14 mg for **3**; 0.48 mmol, 18 mg for **6**; 0.22 mmol, 8 mg for **9**).[9] After being stirred for 15 h at room temperature, 1 equiv of potassium hexafluorophosphate was added to the reaction mixture, and then, the solution was stirred for another 2 h. The reaction mixture was filtered off to remove impurities and then evaporated. The products were isolated from the residue by precipitation from a dichloromethane/diethylether mixture. To improve the purity, the crude products were subjected to chromatography on silica gel using a 9/1 dichloromethane/ethanol mixture. The second fraction was collected and evaporated and the solid dried under vacuum.

*$[(\eta^6\text{-}p\text{-}MeC_6H_4Pr^i)_2Ru_2(\mu\text{-}SC_6H_5)_3]Cl$ (**1**).* Yield: 155 mg (93%). ^1H NMR (400 MHz, $CDCl_3$): δ = 0.77 (d, 6 H, ^3J = 7 Hz, $H_{CH(CH3)2}$), 0.88 (d, 6 H, ^3J = 7 Hz, $H_{CH(CH3)2}$), 1.61 (s, 6 H, H_{CH3}), 1.92 (m, 2 H, $H_{CH(CH3)2}$), 5.10 (d, 2 H, ^3J = 6 Hz, $H_{p\text{-cymene}}$), 5.13 (d, 2 H, ^3J = 6 Hz, $H_{p\text{-cymene}}$), 5.23 (d, 2 H, ^3J = 6 Hz, $H_{p\text{-cymene}}$), 5.52 (m, 2 H, $H_{p\text{-cymene}}$), 7.36−7.41 (m, 9 H, H_{ar}), 7.89 (d, 6 H, ^3J = 7 Hz, H_{ar}) ppm. $^{13}C\{^1H\}$ NMR (100 MHz, $CDCl_3$): δ = 17.71 (C_{CH3}), 21.95 ($C_{CH(CH3)2}$), 22.53 ($C_{CH(CH3)2}$), 30.58 ($C_{CH(CH3)2}$), 83.65 (Ru−C_{ar}), 84.76 (Ru−C_{ar}), 85.03 (Ru−C_{ar}), 85.37 (Ru−C_{ar}), 99.97 (Ru−C_{ar}), 107.39 (Ru−C_{ar}), 128.45 (C_{ar}), 129.19 (C_{ar}), 132.57 (C_{ar}), 137.81 (C_{ar}) ppm. MS (positive mode): m/z = 799.1 $[M - Cl]^+$. Anal. Calcd for $C_{38}H_{43}ClRu_2S_3$ (833.54): C 54.76, H 5.20; Found: C 54.69, H 5.32%. These data are in agreement with those reported by Mashima for $[(\eta^6\text{-}p\text{-}MeC_6H_4Pr^i)_2Ru_2(\mu\text{-}SC_6H_5)_3]Cl$.[10]

*$[(\eta^6\text{-}p\text{-}MeC_6H_4Pr^i)_2Ru_2(\mu\text{-}SeC_6H_5)_3]Cl$ (**2**).* Yield: 105 mg (66%). ^1H NMR (400 MHz, $CDCl_3$): δ = 0.74 (d, 6 H, ^3J = 7 Hz, $H_{CH(CH3)2}$), 0.87 (d, 6 H, ^3J = 7 Hz, $H_{CH(CH3)2}$), 1.72 (s, 6 H, H_{CH3}), 2.08 (m, 2 H, $H_{CH(CH3)2}$), 5.19 (d, 2 H, ^3J = 6 Hz, $H_{p\text{-cymene}}$), 5.25 (d, 2 H, ^3J = 6 Hz, $H_{p\text{-cymene}}$), 5.31 (d, 2 H, ^3J = 6 Hz, $H_{p\text{-cymene}}$), 5.51 (d, 2 H, ^3J = 6 Hz, $H_{p\text{-cymene}}$), 7.31−7.36 (m, 9 H, H_{ar}), 7.75−7.79 (m, 6 H, H_{ar}) ppm. $^{13}C\{^1H\}$ NMR (100 MHz, $CDCl_3$): δ = 18.21 (C_{CH3}), 21.83 ($C_{CH(CH3)2}$), 22.84 ($C_{CH(CH3)2}$), 30.90 ($C_{CH(CH3)2}$), 82.41 (Ru−C_{ar}), 83.43 (Ru−C_{ar}), 83.65 (Ru−C_{ar}), 84.32(Ru−C_{ar}), 99.15 (Ru−C_{ar}),

dx.doi.org/10.1021/ic4022307 | Inorg. Chem. 2013, 52, 13663−13673

107.27 (Ru−C_{ar}), 128.51 (C_{ar}), 129.33 (C_{ar}), 130.34 (C_{ar}), 133.24 (C_{ar}) ppm. $^{77}Se\{^1H\}$ NMR (76.3 MHz, CD_2Cl_2, 25 °C): δ = −140.7 ppm. MS (positive mode): m/z = 939.1 $[M - Cl]^+$. These data are in agreement with those reported by Mashima for $[(\eta^6\text{-}p\text{-}MeC_6H_4Pr^i)_2Ru_2(\mu\text{-}SeC_6H_5)_3]PF_6$.[9]

*$[(\eta^6\text{-}p\text{-}MeC_6H_4Pr^i)_2Ru_2(\mu\text{-}TeC_6H_5)_3]PF_6$ (**3**).* Yield: 74 mg (47%). ^1H NMR (400 MHz, $CDCl_3$): δ = 0.77 (d, 6 H, ^3J = 7 Hz, H $H_{CH(CH3)2}$), 0.90 (d, 6 H, ^3J = 7 Hz, H $H_{CH(CH3)2}$), 1.96 (s, 6 H, H_{CH3}), 2.32−2.35 (m, 2 H, H $H_{CH(CH3)2}$), 5.41 (d, 2 H, ^3J = 6 Hz, $H_{p\text{-cymene}}$), 5.48−5.51 (m, 4 H, $H_{p\text{-cymene}}$), 5.63−5.64 (m, 2 H, $H_{p\text{-cymene}}$), 7.27−7.39 (m, 9 H, H_{ar}), 7.62−7.64 (m, 6 H, H_{ar}) ppm. $^{31}P\{^1H\}$ NMR (162 MHz, CD_2Cl_2) δ = −144.46 (m) ppm. $^{13}C\{^1H\}$ NMR (100 MHz, $CDCl_3$): δ = 19.32 (C_{CH3}), 22.04 ($C_{CH(CH3)2}$), 23.34 ($C_{CH(CH3)2}$), 31.71 ($C_{CH(CH3)2}$), 82.10 (Ru−C_{ar}), 82.70 (Ru−C_{ar}), 83.40 (Ru−C_{ar}), 84.20 (Ru−C_{ar}), 99.81 (Ru−C_{ar}), 109.22 (Ru−C_{ar}), 128.92 (C_{ar}), 129.20 (C_{ar}), 136.70 (C_{ar}) ppm. ESI-MS (positive mode): m/z = 1084.3 $[M - PF_6]^+$. Anal. Calcd for $C_{38}H_{43}F_6PRu_2Te_3{\cdot}2CH_2Cl_2$ (1399.52): C 34.33, H 3.38. Found: C 34.72, H 3.74%. These data are in agreement with those reported by Mashima for $[(\eta^6\text{-}p\text{-}MeC_6H_4Pr^i)_2Ru_2(\mu\text{-}TeC_6H_5)_3]PF_6$.[9]

*$[(\eta^5\text{-}C_5Me_5)_2Rh_2(\mu\text{-}SC_6H_5)_3]Cl$ (**4**).* Yield: 105 mg (77%). ^1H NMR (400 MHz, $CDCl_3$): δ = 1.34 (s, 30 H, C_5Me_5), 7.33−7.37 (m, 9 H, H_{ar}), 7.80−7.81 (m, 6 H, H_{ar}) ppm. $^{13}C\{^1H\}$ NMR (100 MHz, CD_2Cl_2): δ = 8.78 (C_{CH3}), 97.87 (Rh−C_{ar}), 128.83 (C_{ar}), 128.92 (C_{ar}), 132.49 (C_{ar}), 133.24 (C_{ar}) ppm. ESI MS (positive mode): m/z = 803.1 $[M - Cl]^+$. Anal. Calcd for $C_{38}H_{45}ClRh_2S_3{\cdot}2H_2O$ (875.25): C 52.15, H 5.64. Found: C 51.87, H 5.69%.

*$[(\eta^5\text{-}C_5Me_5)_2Rh_2(\mu\text{-}SeC_6H_5)_3]Cl$ (**5**).* Yield: 90 mg (57%). ^1H NMR (400 MHz, $CDCl_3$): δ = 1.49 (S, 30 H, H_{C5Me5}), 7.31−7.34 (m, 6 H, H_{ar}), 7.38−7.42 (m, 3 H, H_{ar}), 7.65−7.67 (m, 6 H, H_{ar}) ppm. $^{13}C\{^1H\}$ NMR (100 MHz, $CDCl_3$): δ = 9.35 (C_{CH3}), 97.77 (Rh−C_{ar}), 125.15 (C_{ar}), 128.98 (C_{ar}), 129.04 (C_{ar}), 134.03 (C_{ar}) ppm. $^{77}Se\{^1H\}$ NMR (76.3 MHz, CD_2Cl_2, 25 °C): δ = −74.2 ($^1J_{Se-Rh}$ = 38.5 Hz) ppm. ESI-MS (positive mode): m/z = 943.9 $[M - Cl]^+$. Anal. Calcd for $C_{38}H_{45}ClRh_2Se_3{\cdot}2H_2O$ (1015.94): C 44.92, H 4.86. Found: C 45.03, H 4.83%.

*$[(\eta^5\text{-}C_5Me_5)_2Rh_2(\mu\text{-}TeC_6H_5)_3]PF_6$ (**6**).* Yield: 102 mg (51%). ^1H NMR (400 MHz, CD_2Cl_2): δ = 1.79 (s, 30 H, H_{C5Me5}), 7.27−7.31 (m, 6 H, H_{ar}), 7.42−7.47 (m, 3 H, H_{ar}), 7.57−7.59 (m, 6 H, H_{ar}) ppm. $^{31}P\{^1H\}$ NMR (162 MHz, CD_2Cl_2): δ = −144.54 (m) ppm. $^{13}C\{^1H\}$ NMR (100 MHz, $CDCl_3$): δ = 10.30 (C_{CH3}), 99.38 (Rh−C_{ar}), 128.97 (C_{ar}), 129.02 (C_{ar}), 129.23 (C_{ar}), 137.77 (C_{ar}) ppm. ESI-MS (positive mode): m/z = 1091.6 $[M - PF_6]^+$. Anal. Calcd for $C_{38}H_{45}F_6PRh_2Te_3$ (1235.34): C 36.95, H 3.67. Found: C 36.87, H 3.81%.

*$[(\eta^5\text{-}C_5Me_5)_2Ir_2(\mu\text{-}SC_6H_5)_3]Cl$ (**7**).* Yield: 100 mg (78%). ^1H NMR (400 MHz, $CDCl_3$): δ =1.38 (s, 30 H, H_{C5Me5}), 7.36−7.38 (m, 9 H, H_{ar}), 7.75−7.78 (m, 6 H, H_{ar}) ppm. $^{13}C\{^1H\}$ NMR (100 MHz, CD_2Cl_2): δ = 8.50 (C_{CH3}), 91.52 (Rh−C_{ar}), 128.75 (C_{ar}), 129.35 (C_{ar}), 130.56 (C_{ar}), 132.99 (C_{ar}) ppm. ESI MS (positive mode): m/z = 982.2 [M - Cl]$^+$. Anal. Calcd for $C_{38}H_{45}ClIr_2S_3{\cdot}2H_2O$ (1053.88): C 43.31, H 4.69. Found: C 43.31, H 4.58%.

*$[(\eta^5\text{-}C_5Me_5)_2Ir_2(\mu\text{-}SeC_6H_5)_3]Cl$ (**8**).* Yield: 91 mg (63%). ^1H NMR (400 MHz, CD_2Cl_2): δ = 1.52 (s, 30 H, H_{C5Me5}), 7.33−7.42 (m, 9 H, H_{ar}), 7.66−7.68 (m, 6 H, H_{ar}) ppm. $^{13}C\{^1H\}$ NMR (100 MHz, CD_2Cl_2): δ = 8.67 (C_{CH3}), 91.36 (Ir−C_{ar}), 124.65 (C_{ar}), 128.80 (C_{ar}), 128.96 (C_{ar}), 133.84 (C_{ar}) ppm. $^{77}Se\{^1H\}$ NMR (76.3 MHz, CD_2Cl_2, 25 °C): δ = −106.0 ppm. ESI-MS (positive mode): m/z = 1123.8 $[M - Cl]^+$. Anal. Calcd for $C_{38}H_{45}ClIr_2Se_3{\cdot}2H_2O$ (1194.56): C 38.21, H 4.13. Found: C 38.60, H 4.21%.

*$[(\eta^5\text{-}C_5Me_5)_2Ir_2(\mu\text{-}TeC_6H_5)_3]PF_6$ (**9**).* Yield: 45 mg (43%). ^1H NMR (400 MHz, CD_2Cl_2): δ = 1.82 (s, 30 H, H_{C5Me5}), 7.28−7.32 (m, 6 H, H_{ar}), 7.38−7.43 (m, 3 H, H_{ar}), 7.57−7.59 (m, 6 H, H_{ar}) ppm. $^{31}P\{^1H\}$ NMR (162 MHz, CD_2Cl_2): δ = −144.55 (m) ppm. $^{13}C\{^1H\}$ NMR (100 MHz, CD_2Cl_2): δ = 9.69 (C_{CH3}), 93.16 (Ir−C_{ar}), 129.07 (C_{ar}), 129.30 (C_{ar}), 137.34 (C_{ar}), 137.45 (C_{ar}) ppm. ESI-MS (positive mode): m/z = 1269.6 $[M - PF_6]^+$. Anal. Calcd for $C_{38}H_{45}F_6Ir_2PTe_3$ (1413.96): C 32.28, H 3.21. Found: C, 32.34; H, 3.48%.

*Preparation of Mixed Chalcogenolato-Bridged Dinuclear Complexes (**10**−**15**). Synthesis of $[(\eta^6\text{-}p\text{-}MeC_6H_4Pr^i)_2Ru_2(\mu\text{-}SeC_6H_5)(\mu\text{-}SCH_2C_6H_4\text{-}p\text{-}Bu^t)_2]Cl$ (**10**), $[(\eta^5\text{-}C_5Me_5)_2Rh_2(\mu\text{-}SeC_6H_5)(\mu\text{-}SCH_2C_6H_5)_2]Cl$ (**12**), and $[(\eta^5\text{-}C_5Me_5)_2Ir_2(\mu\text{-}SeC_6H_5)(\mu\text{-}SCH_2C_6H_5)_2]Cl$ (**14**).* The neutral dinuclear dichlorido complexes $(\eta^6\text{-}p\text{-}MeC_6H_4Pr^i)_2Ru_2Cl_2(\mu\text{-}SCH_2C_6H_4\text{-}p\text{-}Bu^t)_2$ (0.07 mmol, 60 mg for **10**), $(\eta^5\text{-}C_5Me_5)_2Rh_2Cl_2(\mu\text{-}SCH_2C_6H_5)_2$ (0.13 mmol, 100 mg for **12**), or $(\eta^5\text{-}C_5Me_5)_2Ir_2Cl_2(\mu\text{-}SCH_2C_6H_5)_2$ (0.09 mmol, 88 mg for **14**) were dissolved in technical-grade ethanol (20 mL). Then, an ethanolic solution (2.5 mL) of benzeneselenol (0.13 mmol, 14 μL for **10**; 0.25 mmol, 27 μL for **12**; 0.18 mmol, 19 μL for **14**) was added dropwise to the reaction mixture. The reaction was carried out at reflux for 18 h. After this period, ethanol was evaporated, and the salts were isolated from the residue by precipitation from a dichloromethane/hexane solution. After filtration, the residue was washed several times with diethyl ether and hexane and dried under vacuum.

*Synthesis of $[(\eta^6\text{-}p\text{-}MeC_6H_4Pr^i)_2Ru_2(\mu\text{-}TeC_6H_5)(\mu\text{-}SCH_2C_6H_4\text{-}p\text{-}Bu^t)_2]PF_6$ (**11**), $[(\eta^5\text{-}C_5Me_5)_2Rh_2(\mu\text{-}TeC_6H_5)(\mu\text{-}SCH_2C_6H_5)_2]PF_6$ (**13**), and $[(\eta^5\text{-}C_5Me_5)_2Ir_2(\mu\text{-}TeC_6H_5)(\mu\text{-}SCH_2C_6H_5)_2]PF_6$ (**15**).* The dinuclear dichlorido complexes $(\eta^6\text{-}p\text{-}MeC_6H_4Pr^i)_2Ru_2Cl_2(\mu\text{-}SCH_2C_6H_4\text{-}p\text{-}Bu^t)_2$ (0.11 mmol, 100 mg for **11**), $(\eta^5\text{-}C_5Me_5)_2Rh_2Cl_2(\mu\text{-}SCH_2C_6H_5)_2$ (0.13 mmol, 100 mg for **13**), or $(\eta^5\text{-}C_5Me_5)_2Ir_2Cl_2(\mu\text{-}SCH_2C_6H_5)_2$ (0.13 mmol, 125 mg for **15**) were dissolved in technical-grade ethanol (25 mL) and added to an ethanolic solution of sodium tellurophenolate, which was prepared by the treatment of diphenyl ditelluride (0.11 mmol, 45 mg for **11**; 0.13 mmol, 52 mg for **13**; 0.13 mmol, 52 mg for **15**) with sodium borohydride (0.22 mmol, 8 mg for **11**; 0.25 mmol, 38 mg for **13**; 0.26 mmol, 10 mg for **15**).[9] After being stirred for 15 h, 1 equiv of potassium hexafluorophosphate was added to the solution, and the solution was stirred for another 2 h. The reaction mixture was filtered off to remove impurities and the solvent evaporated. The products were isolated from the residue by precipitation from a dichloromethane/diethyl ether mixture. To improve the purity, the crude products were subjected to chromatography on silica gel using a 9/1 dichloromethane/ethanol mixture. The second fraction was collected and evaporated and the solid dried under vacuum.

*$[(\eta^6\text{-}p\text{-}MeC_6H_4Pr^i)_2Ru_2(\mu\text{-}SeC_6H_5)(\mu\text{-}SCH_2C_6H_4\text{-}p\text{-}Bu^t)_2]Cl$ (**10**).* Yield: 40 mg (59%). ^1H NMR (400 MHz, CD_2Cl_2): δ = 0.87 (d, 6 H, ^3J = 7 Hz, $H_{CH(CH3)2}$), 0.96 (d, 6 H, ^3J = 7 Hz, $H_{CH(CH3)2}$), 1.36 (d, 18 H, ^3J = 7 Hz, $H_{(CH3)3}$), 1.82 (s, 6 H, H_{CH3}), 1.91−2.00 (m, 2 H, $H_{CH(CH3)2}$), 3.49 (s, 2 H, H_{CH2}), 3.52 (s, 2 H, H_{CH2}), 4.58 (d, 2 H, ^3J = 6 Hz, $H_{p\text{-cymene}}$), 4.85 (d, 2 H, ^3J = 6 Hz, $H_{p\text{-cymene}}$), 5.06 (d, 2 H, ^3J = 6 Hz, $H_{p\text{-cymene}}$), 5.20 (d, 2 H, ^3J = 6 Hz, $H_{p\text{-cymene}}$), 7.29−7.52 (m, 11 H, H_{ar}), 7.79 (d, 2 H, ^3J = 7 Hz, H_{ar}) ppm. $^{13}C\{^1H\}$ NMR (100 MHz, $CDCl_3$): δ = 18.02 (C_{CH3}), 22.23 ($C_{CH(CH3)2}$), 22.84 ($C_{CH(CH3)2}$), 31.06 ($C_{(CH3)3}$), 34.58 ($C_{CH(CH3)2}$), 40.20 (C_{CH2}), 41.49 (C_{CH2}), 82.10 (Ru−C_{ar}), 82.88 (Ru−C_{ar}), 83.01 (Ru−C_{ar}), 83.52 (Ru−C_{ar}), 100.23 (Ru−C_{ar}), 106.76 (Ru−C_{ar}), 125.47 (C_{ar}), 128.52 (C_{ar}), 128.91 (C_{ar}), 129.23 (C_{ar}), 133.44 (C_{ar}), 136.57 (C_{ar}), 136.92 (C_{ar}), 151.62 (C_{ar}) ppm. $^{77}Se\{^1H\}$ NMR (76.3 MHz, CD_2Cl_2, 25 °C): δ = −142.0 ppm. ESI-MS (positive mode): m/z = 986.4 $[M - Cl]^+$. Anal. Calcd for $C_{48}H_{63}ClRu_2S_2Se{\cdot}CH_2Cl_2$ (1105.09): C 53.23, H 5.93. Found: C 53.62, H 6.20%.

*$[(\eta^6\text{-}p\text{-}MeC_6H_4Pr^i)_2Ru_2(\mu\text{-}TeC_6H_5)(\mu\text{-}SCH_2C_6H_4\text{-}p\text{-}Bu^t)_2]PF_6$ (**11**).* Yield: 86 mg (66%). ^1H NMR (400 MHz, $CDCl_3$): δ = 0.80 (d, 6 H, ^3J = 7 Hz, $H_{CH(CH3)2}$), 0.96 (d, 6 H, ^3J = 7 Hz, $H_{CH(CH3)2}$), 1.34 (d, 18 H, ^3J = 7 Hz, $H_{(CH3)3}$), 1.89 (s, 6 H, H_{CH3}), 2.00−2.08 (m, 2 H, $H_{CH(CH3)2}$), 3.14 (s, 2 H, H_{CH2}), 3.60 (s, 2 H, H_{CH2}), 4.45 (d, 2 H, ^3J = 6 Hz, $H_{p\text{-cymene}}$), 4.77 (d, 2 H, ^3J = 6 Hz, $H_{p\text{-cymene}}$), 5.18 (d, 2 H, ^3J = 6 Hz, $H_{p\text{-cymene}}$), 5.33 (d, 2 H, ^3J = 6 Hz, $H_{p\text{-cymene}}$), 7.20−7.24 (m, 2 H, H_{ar}), 7.33−7.39 (d, 4 H, H_{ar}), 7.41−7.47 (m, 5 H, H_{ar}), 7.72 (d, 2 H, ^3J = 8 Hz, H_{ar}) ppm. $^{31}P\{^1H\}$ NMR (162 MHz, CD_2Cl_2): δ = −144.48 (m) ppm. $^{13}C\{^1H\}$ NMR (100 MHz, $CDCl_3$): δ = 18.45 (C_{CH3}), 22.14 ($C_{CH(CH3)2}$), 22.94 ($C_{CH(CH3)2}$), 31.06 ($C_{(CH3)3}$), 34.60 ($C_{CH(CH3)2}$), 43.45 (C_{CH2}), 44.24 (C_{CH2}), 82.04 (Ru−C_{ar}), 82.33 (Ru−C_{ar}), 83.31 (Ru−C_{ar}), 100.46 (Ru−C_{ar}), 107.12 (Ru−C_{ar}), 107.72 (Ru−C_{ar}), 125.53 (C_{ar}), 128.90 (C_{ar}), 129.18 (C_{ar}), 129.89 (C_{ar}), 136.12 (C_{ar}), 136.98 (C_{ar}), 137.16 (C_{ar}), 151.84 (C_{ar}) ppm. ESI-MS (positive mode): m/z = 1034.6 $[M - PF_6]^+$. Anal. Calcd for $C_{48}H_{63}F_6PRu_2S_2Te{\cdot}2CH_2Cl_2$ (1348.71): C 44.53, H 5.01. Found: C 44.83, H 4.80%.

dx.doi.org/10.1021/ic4022307 | Inorg. Chem. 2013, 52, 13663−13673

[(η^5-C_5Me_5)$_2$Rh$_2$(μ-SeC$_6$H$_5$)(μ-SCH$_2$C$_6$H$_5$)$_2$]Cl (**12**). Yield: 67 mg (58%). ^{1}H NMR (400 MHz, CD_2Cl_2): δ = 1.48 (s, 30 H, H_{CH3}), 3.65 (s, 2 H, H_{CH2}), 3.80 (s, 2 H, H_{CH2}), 7.32−7.37 (m, 4 H, H_{ar}), 7.43−7.47 (m, 5 H, H_{ar}), 7.61 (t, 4 H, ^3J = 8 Hz, H_{ar}), 7.70−7.72 (m, 2 H, H_{ar}) ppm. $^{13}C\{^1H\}$ NMR (100 MHz, CD_2Cl_2): δ = 9.12 (CH_3), 35.93 (CH_2), 36.45(CH_2), 98.11 (Rh−C_{ar}), 125.59 (C_{ar}), 127.47 (C_{ar}), 127.69 (C_{ar}), 128.62 (C_{ar}), 128.90 (C_{ar}), 133.79 (C_{ar}), 139.56 (C_{ar}), 139.64 (C_{ar}) ppm. $^{77}Se\{^1H\}$ NMR (76.3 MHz, CD_2Cl_2, 25 °C): δ = −63.6 ($^1J_{Se-Rh}$ = 40.4 Hz) ppm. ESI-MS (positive mode): m/z = 879.7 $[M - Cl]^+$. Anal. Calcd for $C_{40}H_{49}ClRh_2S_2Se{\cdot}2H_2O$ (950.20): C 50.56, H 5.62. Found: C 50.29, H 5.81%.

[(η^5-C_5Me_5)$_2$Rh$_2$(μ-TeC$_6$H$_5$)(μ-SCH$_2$C$_6$H$_5$)$_2$]PF$_6$ (**13**). Yield: 107 mg (79%). ^{1}H NMR (400 MHz, CD_2Cl_2): δ = 1.57 (s, 30 H, H_{CH3}), 3.39 (s, 2 H, H_{CH2}), 3.91 (s, 2 H, H_{CH2}), 7.28−7.31 (m, 2 H, H_{ar}), 7.34−7.38 (m, 2 H, H_{ar}), 7.42−7.46 (m, 5 H, H_{ar}), 7.53 (d, 2 H, ^3J = 8 Hz, H_{ar}), 7.62 (d, 2 H, ^3J = 8 Hz, H_{ar}), 7.72−7.75 (m, 2 H, H_{ar}) ppm. $^{31}P\{^1H\}$ NMR (162 MHz, CD_2Cl_2): δ = −144.56 (m) ppm. $^{13}C\{^1H\}$ NMR (100 MHz, CD_2Cl_2): δ = 9.59 (C_{CH3}), 37.82 (C_{CH2}), 39.19 (C_{CH2}), 98.59 (Rh−C_{ar}), 127.39 (C_{ar}), 127.77 (C_{ar}), 128.65 (C_{ar}), 129.01 (C_{ar}), 129.45 (C_{ar}), 137.32 (C_{ar}), 139.39 (C_{ar}), 139.82 (C_{ar}) ppm. ESI-MS (positive mode): m/z = 928.1 $[M - PF_6]^+$. Anal. Calcd for $C_{40}H_{49}F_6PRh_2S_2Te$ (1072.32): C 44.80, H 4.61. Found C 44.76, H 4.73%.

[(η^5-C_5Me_5)$_2$Ir$_2$(μ-SeC$_6$H$_5$)(μ-SCH$_2$C$_6$H$_5$)$_2$]Cl (**14**). Yield: 65 mg (66%). ^{1}H NMR (400 MHz, CD_2Cl_2): δ = 1.49 (s, 30 H, H_{CH3}), 3.86 (s, 2 H, H_{CH2}), 4.03 (s, 2 H, H_{CH2}), 7.32−7.39 (m, 4 H, H_{ar}), 7.43−7.47 (m, 5 H, H_{ar}), 7.58 (t, 4 H, ^3J = 8 Hz, H_{ar}), 7.67−7.69 (m, 2 H, H_{ar}) ppm. $^{13}C\{^1H\}$ NMR (100 MHz, CD_2Cl_2): δ = 8.86 (C_{CH3}), 35.85 (C_{CH2}), 37.26 (C_{CH2}), 91.86 (Ir−C_{ar}), 123.28 (C_{ar}), 127.65 (C_{ar}), 127.85 (C_{ar}), 128.72 (C_{ar}), 128.94 (C_{ar}), 129.16 (C_{ar}), 133.32 (C_{ar}), 138.98 (C_{ar}) ppm. $^{77}Se\{^1H\}$ NMR (76.3 MHz, CD_2Cl_2, 25 °C): δ = −81.1 ppm. ESI-MS (positive mode): m/z = 1057.9 $[M - Cl]^+$. Anal. Calcd for $C_{40}H_{49}ClIr_2S_2Se$ (1093.14): C 43.96, H 4.52. Found: C 43.32, H 4.93%.

[(η^5-C_5Me_5)$_2$Ir$_2$(μ-TeC$_6$H$_5$)(μ-SCH$_2$C$_6$H$_5$)$_2$]PF$_6$ (**15**). Yield: 132 mg (82%). ^{1}H NMR (400 MHz, CD_2Cl_2): δ = 1.59 (s, 30 H, H_{CH3}), 3.65 (s, 2 H, H_{CH2}), 4.12 (s, 2 H, H_{CH2}), 7.27−7.31 (m, 2 H, H_{ar}), 7.35−7.39 (m, 2 H, H_{ar}), 7.41−7.46 (m, 5 H, H_{ar}), 7.50−7.52 (m, 2 H, H_{ar}), 7.58−7.60 (d, 2 H, H_{ar}), 7.70−7.72 (m, 2 H, H_{ar}) ppm. $^{31}P\{^1H\}$ NMR (162 MHz, CD_2Cl_2): δ = −144.55 (m) ppm. $^{13}C\{^1H\}$ NMR (100 MHz, CD_2Cl_2): δ = 9.24 (C_{CH3}), 39.76 (C_{CH2}), 40.84 (C_{CH2}), 92.47 (Ir−C_{ar}), 127.59 (C_{ar}), 127.97 (C_{ar}), 128.59 (C_{ar}), 128.80 (C_{ar}), 129.50 (C_{ar}), 137.08 (C_{ar}), 138.93 (C_{ar}), 139.07 (C_{ar}) ppm. ESI-MS (positive mode): m/z = 1106.1 $[M - PF_6]^+$. Anal. Calcd for $C_{40}H_{49}F_6Ir_2PS_2Te$ (1250.95): C 38.41, H 3.95. Found: C 38.40, H 4.02%.

MTT Assays. In order to find the half maximal inhibitory concentration (IC_{50}) of each complex with normal human cell lines (CRL-2115, CRL-2120) and human cancer cell lines (MCF-7, B16F10, and A549), cells were cultured according to the supplier's recommendations. To study the cytotoxicity of the complexes, after 80% confluence, cells were trypsinized with 0.1% trypsin-EDTA and harvested by centrifugation at 500*g*. Serial dilutions of cells were made from 1 × 10^6 to 1 × 10^3 cells per mL. The cells were seeded in triplicate in a 96 well plate. The suspended cells were treated for 24 h with 10 nM, 50 nM, 100 nM, 300 nM, 500 nM, 1 μM, and 2 μM of each complex. Normal as well as cancer cells to which no complex were added served as controls. After incubation, MTT (100 μL, 5 mg/mL) solution was added to each well, and the cell viability was determined by measuring the ability of cells to transform MTT to a purple formazan dye. The absorbance of samples at 570 nm was measured using a UV−vis spectrophotometer. Percentage of viable cells was calculated using the formula given below.

$$\text{percentage of cell viability} = \frac{OD_{570}\ \text{sample}}{OD_{570}\ \text{control}} \times 100$$

Here, the OD_{570} (sample) corresponds to absorbance obtained from the wells treated with complexes and the OD_{570} (control) represents the absorbance from the wells in which no complex was added.

The melting experiments were carried out using UV−vis spectrophotometer (Lambda 35, ABI) with a water bath attached to control the temperature. CT-DNA and each complex concentration were maintained at 25 μM in the cuvette. The variation of the CT-DNA absorbance at 260 nm was recorded and plotted versus the temperature.

Cell Viability Assays. Normal and cancer cell lines were seeded at 20 000−40 000 cells/cm^2 with 0.2 mL/cm^2 media and incubated for 48 h at 37 °C, 6% CO_2, 95% relative humidity. All cells were treated with complexes at 300 nM concentrations. After 24 h of incubation, cells were washed with 300 μL PBS or 0.02% EDTA and trypsinized, followed by harvesting at 37 °C. A 200 μL cell suspension was transferred into a 1.5 mL microcentrifuge tube. To the cell suspension, 300 μL of PBS followed by 500 μL of 0.4% trypan blue solutions were added. To get a homogenized solution, the microcentrifuge tube was gently tapped for 5 min, and 20 μL of cell suspension was loaded into a chamber of the hemocytometer for measurements.

Statistical Analyzes. The results obtained from cell viability and MTT assays were subjected to statistical analyses. The SPSS statistic software (Version 18.0, Chicago, IL) was used for all statistical analyses. The statistical parameters like mean value and standard deviation were calculated using descriptive statistics. Data were considered significant with p value $\leq$0.05.

Flow Cytometry and Confocal Microscopy Studies. Since MTT and cell culture assays yielded encouraging results with B16F10 cells, they were considered for confocal and flow cytometry experiments. Cell cycle assay was performed by following the protocol reported by Angelis et al..[26] After 70% confluence, the cells were treated with 300 nM concentration of each complexes, for 3 h. Then, 1 × 10^6 cells were washed with 2× binding buffer and resuspended in 100 μL binding buffer and Annexin-V-FITC from Abcam (1.0 μg). The cells were then incubated at room temperature for 10 min, followed by the addition of 400 μL of binding buffer containing 1 μL of propidium iodide (PI) from Sigma-Aldrich. Stained cells were analyzed using FACS Calibur flow cytometer from B.D. Biosceinces. Annexin-V-FITC and PI labeled cells were excited using a 488 nm solid-state laser, and fluorescence emission intensity of FITC and PI were captured using 530/30 and 585/42 band-pass filters, respectively.

For confocal microscopic studies, B16F10 cells were rinsed with 1X PBS and incubated with 2.5% formaldehyde in PBS for 10 min at room temperature, followed by permeabilization with 0.5% Triton X-100 for 5 min. The fixed cells were incubated with 10% FCS in PBS for 1 h at room temperature. The culture plate was then washed with 1X PBS and placed in mounting medium (Vectashield), containing antifade reagent with 300 nM DAPI and incubated for 1−5 min. The cells were rinsed with PBS several times and observed using a fluorescent microscope.

DNA Fragmentation Assays. B16F10 cells were seeded (1 × 10^6) in six-well plates. After 24 h of incubation, cells were treated with 300 nM of complexes **1**, **4**, and **7** (at half maximal inhibitory concentration). After 24 h of treatment, cells were collected and centrifuged at 2500 rpm for 5 min at 4 °C. Pellet was collected and washed with phosphate buffered saline (PBS). Then, 100 μL of lysis buffer was added and centrifuged at 3000 rpm for 5 min at 4 °C, and the supernatant was collected. To the mixture, 10 μL of 10% SDS and 10 μL of (50 mg/mL) RNaseA were added and incubated for 2 h at 56 °C. After incubation, Proteinase K (25 mg/mL) was added, and the cells were incubated at 37 °C for an additional 2 h. Further 65 μL of 10 M ammonium acetate and 500 μL of ice cold ethanol were added and mixed well. Then, these samples were incubated at 80 °C for 1 h. The incubated samples were centrifuged at 12 000 rpm for 20 min at 4 °C, washed with 80% ethanol, and air-dried for 10 min at room temperature. The pellets were dissolved in 50 μL of TE buffer, and electrophoresis was carried out using 2% agarose gel in a TE buffer.

DNA−Complex Interaction Studies. UV−vis titrations were performed using a Lambda 35 spectrophotometer (ABI). The stock solutions of CT-DNA (obtained from Sigma-Aldrich) and of the complexes were prepared in the BPES buffer. Equal aliquots of CT-DNA (50 μM) solution were added to 25 μM solution of the complex in a quartz cuvette. Absorbance spectra were collected from 200 to 400

dx.doi.org/10.1021/ic4022307 | *Inorg. Chem.* 2013, 52, 13663−13673

nm after each addition of CT-DNA into the **1**, **4**, and **7** solutions of the complexes. Titration was performed until the absorption bands of the complex remained intact. Each titration was repeated twice to minimize errors.

CD analyses were performed using a JASCO 815 CD spectrometer (Jasco, Tokyo, Japan) equipped with a 1 cm path length quartz cuvette. All CD measurements and titrations were performed at 25 °C in 100 mM KBPES buffer (pH 7.0) with spectra collected over a wavelength range 200−400 nm. The CT-DNA concentration was maintained at 50 μM and titrated by adding fixed aliquots of the complexes **1**, **4**, and **7** (100 μM stock solutions) to the CT-DNA solution. CD spectra were collected at stoichiometry values (CT-DNA/complex) 1/0 and 1/1 for each complex.

DNA Photocleavage Assays. This experiment was carried out according to the protocol reported by Toshima et al.[27] About 0.5 μg of pBR322 plasmid DNA was taken in Tris-HCl buffer (50 mM, pH 7.5), and 100 μM of complexes **1**, **4**, and **7** were added with the total volume maintained at 20 μL. The DNA samples with complexes were taken in TPP tissue culture test plates and irradiated with UV light (8 W, 365 nm, 4 cm distance) for 1 h. DNA alone (without any complex) was considered as control. To assess ROS generating potential of each complex, a set of samples containing the same quantity of DNA and of complexes (**1**, **4**, and **7**) were irradiated with UV light for 1 h in the presence of the singlet oxygen quencher NaN_3 (100 μM). After irradiation, the samples were collected and mixed with 2 μL of loading dye (50% sucrose and 0.25% bromophenol blue). Then, samples were analyzed by gel electrophoresis on a 0.8% agarose horizontal slab gel containing 0.5 μg/mL ethidium bromide in Tris-EDTA buffer (40 mM Tris, 20 mM acetic acid, and 1 mM EDTA, pH 8.0) at 10 V cm^{-1}.

AUTHOR INFORMATION

Corresponding Authors

*E-mail: bruno.therrien@unine.ch. Phone: +41 (0)32 718 2499. Fax: +41 (0)32 718 2511.

*E-mail: nagesh@ccmb.res.in. Phone: +91 402 7192568. Fax: +91 402 7160311.

Notes

The authors declare no competing financial interest.

ACKNOWLEDGMENTS

J.P.J. and G.G. gratefully thank the Swiss Commission of Fellowship for financial support. B.T. and N.N. thank the Indo Swiss Joint Research Programme (ISJRP) for financial support (Grant CH: 138844) and the Johnson Matthey Research Centre for a generous loan of rhodium, iridium, and ruthenium chloride hydrates.

REFERENCES

(1) Letavayová, L.; Vlčková, V.; Brozmanová, J. *Toxicology* **2006**, *227*, 1−14.

(2) Pia Rigobello, M.; Gandin, V.; Folda, A.; Rundlöf, A.-K.; Fernandes, A. P.; Bindoli, A.; Marzano, C.; Björnstedt, M. *Free Radical Biol. Med.* **2009**, *47*, 710−721.

(3) (a) Rosenberg, B.; Vancamp, L.; Trosko, J. E.; Mansour, V. H. *Nature* **1969**, *222*, 385−386. (b) Hoeschele, J. D. *Dalton Trans.* **2009**, 10648−10650.

(4) Baldew, G. S.; van den Hamer, C. J. A.; Los, G.; Vermeulen, N. P. E.; de Goeji, J. J. M.; Gordon McVie, J. *Cancer Res.* **1989**, *49*, 3020−2023.

(5) (a) Cunha, R. L. O. R.; Gouvea, I. E.; Juliano, L. *An. Acad. Bras. Cienc.* **2009**, *81*, 393−407. (b) Tiekink, E. R. T. *Dalton Trans.* **2012**, *41*, 6390−6395.

(6) (a) Gras, M.; Therrien, B.; Süss-Fink, G.; Zava, O.; Dyson, P. J. *Dalton Trans.* **2010**, *39*, 10305−10313. (b) Ibao, A.-F.; Gras, M.; Therrien, B.; Süss-Fink, G.; Zava, O.; Dyson, P. J. *Eur. J. Inorg. Chem.* **2012**, 1531−1535. (c) Giannini, F.; Furrer, J.; Ibao, A.-F.; Süss-Fink, G.; Therrien, B.; Zava, O.; Baquie, M.; Dyson, P. J.; Štěpnička, P. *JBIC, J. Biol. Inorg. Chem.* **2012**, *17*, 951−960. (d) Giannini, F.; Furrer, J.; Süss-Fink, G.; Clavel, C. M.; Dyson, P. J. *J. Organomet. Chem.* **2013**, *744*, 41−48.

(7) Gupta, G.; Garci, A.; Murray, B. S.; Dyson, P. J.; Fabre, G.; Trouillas, P.; Giannini, F.; Furrer, J.; Süss-Fink, G.; Therrien, B. *Dalton Trans.* **2013**, *42*, 15457−15463.

(8) (a) Chérioux, F.; Thomas, C. M.; Therrien, B.; Süss-Fink, G. *Chem.—Eur. J.* **2002**, *8*, 4377−4382. (b) Chérioux, F.; Thomas, C. M.; Monnier, T.; Süss-Fink, G. *Polyhedron* **2003**, *22*, 543−548. (c) Chérioux, F.; Therrien, B.; Süss-Fink, G. *Eur. J. Inorg. Chem.* **2003**, 1043−1047. (d) Chérioux, F.; Therrien, B.; Süss-Fink, G. *Inorg. Chim. Acta* **2004**, *357*, 834−838. (e) Tschan, M. J.-L.; Chérioux, F.; Therrien, B.; Süss-Fink, G. *Eur. J. Inorg. Chem.* **2004**, 2405−2411. (f) Chérioux, F.; Therrien, B.; Sadki, S.; Comminges, C.; Süss-Fink, G. *J. Organomet. Chem.* **2005**, *690*, 2365−2371. (g) Boudreau, J.; Grenier-Desbiens, J.; Fontaine, F.-G. *Eur. J. Inorg. Chem.* **2010**, 2158−2164.

(9) Mashima, K.; Kaneko, S.; Tani, K.; Kaneyoshi, H.; Nakamura, A. *J. Organomet. Chem.* **1997**, *545*−*546*, 345−356.

(10) Mashima, K.; Mikami, A.; Nakamura, A. *Chem. Lett.* **1992**, *21*, 1795−1798.

(11) Han, W. S.; Lee, S. W. *Bull. Korean Chem. Soc.* **2003**, *24*, 641−644.

(12) Herberhold, M.; Keller, M.; Kremnitz, W.; Daniel, T.; Milius, W.; Wrackmeyer, B.; Nöth, H. *Z. Anorg. Allg. Chem.* **1998**, *624*, 1324−1328.

(13) Mosmann, T. *J. Immunol. Methods* **1983**, *65*, 55−63.

(14) (a) Harris, A. L.; Yang, X.; Hegmans, A.; Povirk, L.; Ryan, J. J.; Kelland, L.; Farrell, N. P. *Inorg. Chem.* **2005**, *44*, 9598−9600. (b) Therrien, B.; Süss-Fink, G.; Govindaswamy, P.; Renfrew, A. K.; Dyson, P. J. *Angew. Chem., Int. Ed.* **2008**, *47*, 3773−3776.

(15) Xu, K.; Liang, X.; Wang, F.; Xie, L.; Xu, Y.; Liu, J.; Qian, X. *Anti-Cancer Drugs* **2011**, *22*, 875−885.

(16) (a) Schwartz, L. M.; Smith, S. W.; Jones, M. E. E.; Osborne, B. A. *Proc. Natl. Acad. Sci. U.S.A.* **1993**, *90*, 980−984. (b) Taimen, P.; Kallajoki, M. *J. Cell Sci.* **2003**, *116*, 571−583.

(17) Ramakrishnan, S.; Palaniandavar, M. *J. Chem. Sci.* **2005**, *117*, 179−186.

(18) Wang, B.-D.; Yang, Z.-Y.; Crewdson, P.; Wang, D.-Q. *J. Inorg. Biochem.* **2007**, *101*, 1492−1504.

(19) Arjmand, F.; Aziz, M. *Eur. J. Med. Chem.* **2009**, *44*, 834−844.

(20) Parkinson, G. N.; Ghosh, R.; Neidle, S. *Biochemistry* **2007**, *46*, 2390−2397.

(21) Satyanarayana, S.; Dabrowiak, J. C.; Chaires, J. B. *Biochemistry* **1993**, *32*, 2573−2584.

(22) Pratviel, G.; Bernadou, J.; Meunier, B. *Adv. Inorg. Chem.* **1998**, *45*, 251−312.

(23) Bennett, M. A.; Smith, A. K. *J. Chem. Soc., Dalton Trans.* **1974**, *2*, 233−241.

(24) (a) Kang, J. W.; Moseley, K.; Maitlis, P. M. *J. Am. Chem. Soc.* **1969**, *91*, 5970−5977. (b) White, C.; Yates, A.; Maitlis, P. M.; Heinekey, D. M. *Inorg. Synth.* **1992**, *29*, 228−234.

(25) Nishio, M.; Matsuzaka, H.; Mizobe, Y.; Hidai, M. *Inorg. Chim. Acta* **1997**, *263*, 119−123.

(26) De Angelis, P. M.; Svendsrud, D. H.; Kravik, K. L.; Stokke, T. *Mol. Cancer* **2006**, *5*, 1−25.

(27) Toshima, K.; Okuno, Y.; Nakajima, Y.; Matsumura, S. *Bioorg. Med. Chem. Lett.* **2002**, *12*, 671−673.